JACS
JOURNAL OF THE AMERICAN CHEMICAL SOCIETY

Communication

pubs.acs.org/JACS

Self-Supported Nanoporous Cobalt Phosphide Nanowire Arrays: An Efficient 3D Hydrogen-Evolving Cathode over the Wide Range of pH 0−14

Jingqi Tian,[†,‡] Qian Liu,[†] Abdullah M. Asiri,[§,∥] and Xuping Sun*[,†,§,∥]

[†]State Key Lab of Electroanalytical Chemistry, Changchun Institute of Applied Chemistry, Chinese Academy of Sciences, Changchun 130022, Jilin, China

[‡]Graduate School of the Chinese Academy of Sciences, Beijing 100039, China

[§]Chemistry Department, Faculty of Science, and [∥]Center of Excellence for Advanced Materials Research, King Abdulaziz University, Jeddah 21589, Saudi Arabia

Supporting Information

ABSTRACT: In this Communication, we report the topotactic fabrication of self-supported nanoporous cobalt phosphide nanowire arrays on carbon cloth (CoP/CC) via low-temperature phosphidation of the corresponding Co(OH)F/CC precursor. The CoP/CC, as a robust integrated 3D hydrogen-evolving cathode, shows a low onset overpotential of 38 mV and a small Tafel slope of 51 mV dec^{-1}, and it maintains its catalytic activity for at least 80 000 s in acidic media. It needs overpotentials (η) of 67, 100, and 204 mV to attain current densities of 10, 20, and 100 mA cm^{-2}, respectively. Additionally, this electrode offers excellent catalytic performance and durability under neutral and basic conditions.

Depletion of fossil fuels and increased environmental concerns have triggered an urgent demand for clean and sustainable alternative energy sources.[1] Hydrogen, as an abundant and renewable clean fuel, is an ideal candidate for replacing fossil fuels in the future.[2] Water electrolysis requires effective electrocatalysts for the hydrogen evolution reaction (HER) to attain high current density at low overpotential. Pt is the best HER catalyst, but its high cost limits its widespread use.[3] The strongly acidic conditions in proton exchange membrane (PEM) technology necessitate acid-stable HER catalysts for PEM-based electrolysis units.[4] The microbial electrolysis cell (MEC), a promising technology for producing hydrogen from wastewater through degradation of organic waste by microbes, requires HER catalysts that operate under neutral conditions.[5] Alkaline water electrolysis, on the other hand, needs catalysts that operate in basic media.[6] As such, developing efficient and inexpensive HER catalysts working at all pH values is highly desirable but remains challenging.

Cobalt has emerged as an interesting non-noble metal for its catalytic power toward hydrogen evolution, and great efforts have been devoted to developing Co-based complexes as HER catalysts in the past years.[7] Practical application of these molecular catalysts requires their grafting onto electrode materials operating with fully aqueous electrolytes,[8] which, however, is a challenge task because of issues with the synthesis of such complexes.[7d] This problem can be effectively solved by directly growing the active phases on current collectors. Indeed, Co-based nanoparticle (H_2-CoCat) and Co-S films have been deposited electrochemically on fluorine-doped tin oxide (FTO) substrates as hydrogen-evolving cathodes.[9] The H_2-CoCat/FTO only works in neutral solutions with moderate activity.[9a] The Co-S/FTO shows high activity in neutral solutions, but it has low activity under alkaline conditions and is not stable in acidic media.[9b] More recently, Kong et al. developed a high-performance, acid-stable 3D hydrogen-evolving cathode composed of $CoSe_2$ nanoparticles grown on carbon fiber paper ($CoSe_2$ NP/CP) via selenization of the corresponding cobalt oxide/CP precursor.[10] Indeed, solar water-splitting devices frequently use 3D electrodes with complicated geometry.[2c,10] Carbon cloth (CC) is highly conductive and flexible, offering us a new 3D support to integrate HER catalysts for application in technological devices. Herein, we describe our recent efforts in developing self-supported nanoporous cobalt phosphide nanowire arrays on CC (CoP/CC) through a topotactic conversion reaction via low-temperature phosphidation of their Co(OH)F/CC precursor.[11] When used as a robust integrated 3D hydrogen-evolving cathode, the CoP/CC shows a low onset overpotential (η) of 38 mV, a small Tafel slope of 51 mV dec^{-1}, and long-term stability in acidic media. It needs overpotentials of 67, 100, and 204 mV to drive current densities of 10, 20, and 100 mA cm^{-2}, respectively. It also offers excellent catalytic activity and durability under neutral and basic conditions.

The CoP/CC was fabricated by low-temperature phosphidation of hydrothermally obtained Co(OH)F/CC precursor.[11] After being coated with Co(OH)F, the CC turned from dark gray to pink; the color of the coated CC further changed to black after phosphidation (Figure S1). Figure 1a shows the X-ray diffraction (XRD) patterns for Co(OH)F and phosphided product scratched down from CC. The diffraction peaks for the Co precursor (red curve) can be well ascribed to the Co(OH)F phase with an orthorhombic structure (JCPDS No. 50-0827), consistent with a previous report.[12] In contrast, the phosphided product shows diffraction peaks (black curve) corresponding to

Received: April 4, 2014
Published: May 15, 2014

dx.doi.org/10.1021/ja503372r | J. Am. Chem. Soc. 2014, 136, 7587−7590

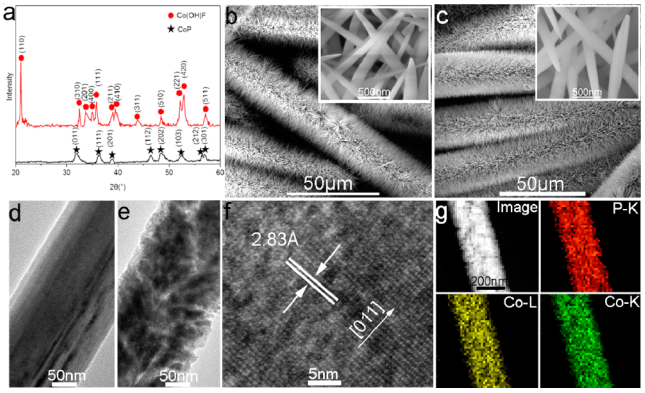

Figure 1. (a) XRD patterns of Co(OH)F and CoP. (b) Low- and (inset) high-magnification SEM images of Co(OH)F/CC, suggesting full coverage of the CC with Co(OH)F nanowire arrays. (c) Low- and (inset) high-magnification SEM images of CoP/CC. TEM images of (d) Co(OH)F and (e) CoP nanowire. (f) HRTEM image of CoP nanowire. (g) STEM image and EDX elemental mapping of P and Co for the CoP nanowire.

orthorhombic CoP (JCPDS No. 29-0497), suggesting successful conversion of Co(OH)F into CoP.

Figure 1b shows a low-magnification scanning electron microscopy (SEM) image of Co(OH)F/CC, indicating the entire surface of the CC was uniformly coated with Co(OH)F nanowires. The high-magnification SEM image (inset) further reveals that such nanowires have diameters of about 100−200 nm and are a few micrometers in length. Following phosphidation, the SEM images show that the 1D morphology was intact (Figure 1c). The corresponding energy-dispersive X-ray (EDX) spectrum (Figure S2a) verifies the 1:1 atomic ratio between Co and P (other peaks originated from the carbon-coated copper grid substrate). The diffraction rings in the selected area electron diffraction (SAED) pattern (Figure S2b) recorded from the CoP nanowires can be identified as the (011), (111), (202), (103), and (301) planes of an orthorhombic CoP structure.[13] Figure 1d shows the transmission electron microscopy (TEM) image of the Co(OH)F nanowire, revealing that it is solid with a smooth surface. The CoP nanowire, however, is porous with a rough surface (Figure 1e), which could arise from the gas release and dehydration of the precursor during annealing.[12] The nitrogen adsorption/desorption isotherm of the CoP nanowires (Figure S3) suggests a Brunauer−Emmett−Teller (BET) surface area of about 36.5 m^2 g^{-1}. The Barrett−Joyner−Halenda (BJH) pore-size distribution curve (inset) shows a broad peak ranging from 8 to 12 nm and two narrow peaks at 2.0 and 4.5 nm, confirming the nanoporous nature of CoP nanowires. The high-resolution TEM (HRTEM) image (Figure 1f) shows that CoP has a lattice fringe with interplane spacing of 0.283 nm, corresponding to the (011) plane of CoP.[13] Figure 1g shows the scanning TEM (STEM) image and the corresponding EDX elemental mapping images of P and Co for a CoP nanowire, further revealing that it is porous in nature and both P and Co elements are uniformly distributed in the whole nanowire. Notably, our CoP/CC is robust enough to withstand a violent 30 min sonication process (Figure S4). SEM observations indicate it preserves its 3D configuration and morphological integrity after 2 h of continuous cyclic voltammetry (CV) scanning at all pH values (Figure S5). XRD analysis further suggests there is no change in the crystalline structure of CoP after electrochemical experiments (Figure S6). These observations imply the high stability of CoP/CC.

Figure 2a shows the polarization curve of CoP/CC (CoP loading: 0.92 mg cm^{-2}) in 0.5 M H_2SO_4 with a scan rate of 2

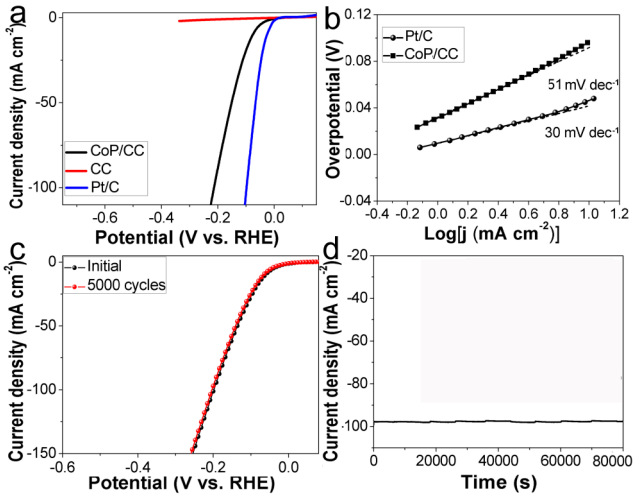

Figure 2. (a) Polarization curves of CoP/CC, blank CC, and Pt/C in 0.5 M H_2SO_4 with a scan rate of 2 mV s^{-1}. (b) Tafel plots of CoP/CC and Pt/C. (c) Polarization curves of CoP/CC initially and after 5000 CV scans between +0.1 and −0.3 V vs RHE. (d) Time-dependent current density curve for CoP/CC under static overpotential of 200 mV for 80 000 s.

mV s^{-1}. Commercial Pt/C and blank CC were also examined for comparison. As expected, Pt/C shows superior HER activity with negligible overpotential. Although blank CC shows poor HER activity even at a potential of −0.4 V, CoP/CC shows an onset overpotential as low as 38 mV, and further negative potential causes a rapid rise of cathodic current, suggesting CoP/CC acts as a high-performance 3D cathode for generating hydrogen from water. This overpotential compares favorably to that of non-Pt HER catalysts in acidic media (Table S1). In addition, this electrode needs overpotentials of 67, 100, and 204 mV to drive current densities of 10, 20, and 100 mA cm^{-2}, respectively. These overpotentials compare favorably to most reported values for non-Pt HER catalysts in acidic aqueous media (Table S1). Note that the CoP loading can be tuned by using different concentrations of the reactants for hydrothermal preparation of Co(OH)F precursor; other loadings of 0.41, 0.68, and 1.28 mg cm^{-2} show inferior catalytic activity (Figure S7), suggesting 0.92 mg cm^{-2} is the optimal loading in our system.

Tafel plots are shown in Figure 2b. The measured value for Pt/C is about 30 mV dec^{-1}, which is consistent with the reported values.[14] The CoP/CC exhibits a small Tafel slope of ∼51 mV dec^{-1} in the region of η = 5−60 mV, which is comparable to or even smaller than those of many acid-stable Mo-based HER catalysts (Table S1). This Tafel slope reveals the HER proceeds via a Volmer−Heyrovsky mechanism.[15] The value of exchange current density of CoP/CC is calculated to be 0.288 mA cm^{-2} by extrapolating the Tafel plot (Figure S8). This value is the largest among non-Pt HER catalysts listed in Table S1. Such high catalytic performance for the CoP nanowires could be rationalized as follows: (1) Their intimate contact with CC enables good mechanical adhesion and electrical connection, facilitating the flow of electrons from CC to CoP during cathodic polarization. (2) CoP, as a good

dx.doi.org/10.1021/ja503372r | J. Am. Chem. Soc. 2014, 136, 7587−7590

conductor of electricity,[16] favors fast electron transport along the nanowire. (3) The porosity of the nanowires not only leads to the exposure of more active sites but also facilitates sufficient transport of reactants and products.[17] (4) The 3D configuration of CoP/CC ensures loose textures and open spaces between neighboring nanoporous CoP nanowires, allowing for easy diffusion of electrolyte into all the pores and thus more efficient use of active sites in CoP. Figure S9 shows a schematic diagram to illustrate the operating principle of the HER based on CoP/CC.

We further examined the durability of CoP/CC. After continuous CV scanning for 5000 cycles in 0.5 M H_2SO_4 at a scan rate of 100 mV s^{-1}, the polarization curve shows negligible difference compared with the initial one (Figure 2c), suggesting superior stability of CoP/CC in the long-term electrochemical process. The time-dependent current density curve under a static overpotential of 200 mV (Figure 2d) suggests CoP/CC maintains its catalytic activity for at least 80 000 s.

The rough estimation of turnover frequency (TOF) for each active site makes it possible to compare the activity of CoP with that of other catalysts. We thus attempted to quantify the active sites by electrochemistry.[18] Figure S10a shows the CVs in the region of −0.2 to 0.6 V vs RHE for CoP/CC at pH 7. While it is difficult to assign the observed peaks to a given redox couple, the integrated charge over the whole potential range should be proportional to the total number of active sites. Assuming a one-electron process for both reduction and oxidation, the upper limit of active sites could be calculated. Figure S10b shows the polarization curve at pH 0, normalized by the active sites and expressed in terms of TOF. As the most active catalyst, Pt shows a TOF of 0.8 s^{-1} at η = 0 mV.[19] To achieve a TOF of 0.725 s^{-1}, CoP/CC needs an overpotential of ∼75 mV, much smaller than that required for defect-rich MoS_2 (300 mV).[20] Pt shows a TOF of 1.73 s^{-1} at an overpotential of 75 mV (Figure S10). To reach a TOF of 4 s^{-1}, this CoP/CC electrode needs an overpotential of 240 mV, 32 mV smaller than that used by core−shell MoO_3−MoS_2 nanowires on FTO (272 mV).[21]

We further investigated the HER performance of the CoP/CC in 1.0 M PBS (pH 7). It shows an onset overpotential of 45 mV and a Tafel slope of 93 mV dec^{-1} with excellent durability (Figure 3a,c). These values compare favorably to most reported values for non-Pt HER catalysts in neutral solutions (Table S2). To attain a current density of 2 mA cm^{-2}, the CoP/CC needs an overpotential of 65 mV, much lower than that required by other HER catalysts (Table S2). The CoP/CC also exhibits high activity under alkaline conditions. Figure 3b shows the polarization curve of CoP/CC in 1.0 M KOH (pH 14). Overpotentials of 115 and 209 mV are required for CoP/CC to approach current densities of 1 and 10 mA cm^{-2}, respectively. These values are much lower than those used by other non-noble metal HER catalysts in basic media, listed in Table S3. CoP/CC still shows good durability even under such alkaline conditions (Figure 3b). The Tafel slope is calculated to be 129 mV dec^{-1} (Figure 3d). Additionally, the CoP/CC electrode shows Faradaic efficiency close to 100% for hydrogen evolution at all pH values (Figure S11).

Figure S12a,b shows X-ray photoelectron spectroscopy (XPS) in the Co(2p) and P(2p) regions for a CoP sample. Two peaks are apparent in the Co(2p) region at 779.1 and 781.8 eV, along with two peaks in the P(2p) region at 129.7 and 134.4 eV. The peaks at 779.1 and 129.7 eV are close to the binding energies (BEs) for Co and P in CoP.[22] The peaks at

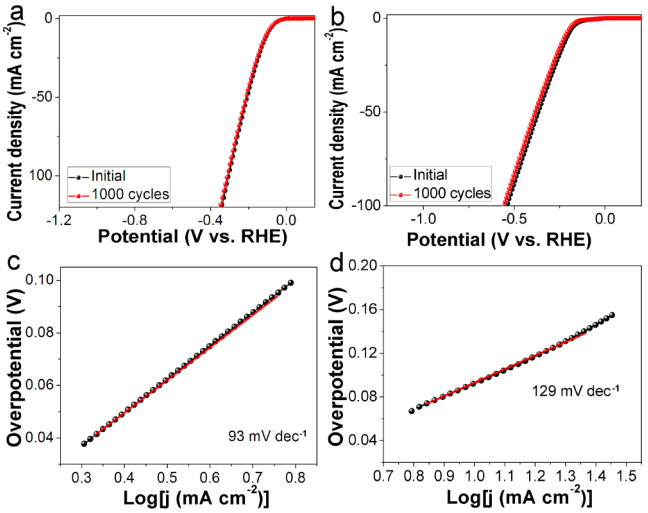

Figure 3. Polarization curves of CoP/CC in (a) 1.0 M PBS (pH 7) and (b) 1.0 M KOH (pH 14) with a scan rate of 2 mV s^{-1}. (c,d) The corresponding Tafel plots.

781.8 and 134.4 eV are assigned to oxidized Co and P species resulting from superficial oxidation of CoP.[23] The survey spectrum (Figure S12c) also confirms the existence of oxygen in the sample. The Co 2p BE of 779.1 eV is positively shifted from that of Co metal (778.1−778.2 eV), and the P 2p BE of 129.7 eV is negatively shifted from that of elemental P (130.2 eV).[24] It suggests the Co in CoP has a partial positive charge (δ^+) while the P has a partial negative charge (δ^-), implying transfer of electron density from Co to P.[22,25] Previous calculations and electron density maps indicate covalency for Co−P bonds with charge separation due to charge transfer from Co to P.[22,26] Metal complex HER catalyst incorporates proton relays from pendant acid−base groups positioned close to the metal center where hydrogen production occurs,[27] and the active sites for hydrogenases also feature pendant bases proximate to the metal centers.[28] Like metal complex catalysts and hydrogenases, the CoP nanowire is also rich with metal center Co (δ^+), with pendant base P (δ^-) close to it, and thus is expected to share the same catalytic mechanism as the metal complex catalysts and hydrogenases toward the HER. For CoP, the Co and basic P function as the hydride-acceptor and proton-acceptor centers, respectively, which facilitates the HER.[14,29] During cathodic polarization, the electrons can be easily transferred to CoP from CC due to their intimate contact, leading to the formation of the hydride at the Co center, like metal complex catalysts.[30] The P could also facilitate the formation of Co-hydride for subsequent hydrogen evolution via electrochemical desorption.[31]

In summary, self-supported nanoporous CoP nanowire arrays on CC are derived successfully via topotactic low-temperature phosphidation of their Co(OH)F/CC precursor. As an 3D hydrogen-evolving cathode, the CoP/CC operates over the pH range 0−14 with excellent catalytic performance, stability, and durability. The whole fabrication process is low cost and easy to scale-up. All these remarkable features, together with the flexible nature of CoP/CC, promise its practical use in technological devices. This study should open up exciting new avenues to explore the design of self-supported 3D electrodes made of transition metal phosphides for HER and other applications.

dx.doi.org/10.1021/ja503372r | J. Am. Chem. Soc. 2014, 136, 7587−7590

■ ASSOCIATED CONTENT

Supporting Information

Experimental details; optical photograph; EDX and XPS spectra; SAED pattern; nitrogen adsorption/desorption isotherm and BJH pore-size distribution curve; SEM images; XRD patterns; Tables S1−S3; polarization curves; exchange current density calculation; schematic diagram; TOF calculation; FE determination. This material is available free of charge via the Internet at http://pubs.acs.org.

■ AUTHOR INFORMATION

Corresponding Author

sunxp@ciac.ac.cn

Notes

The authors declare no competing financial interest.

■ ACKNOWLEDGMENTS

This work was supported by the National Natural Science Foundation of China (No. 21175129) and the National Basic Research Program of China (No.2011CB935800).

■ REFERENCES

(1) (a) Bard, A. J.; Fox, M. A. *Acc. Chem. Res.* **1995**, *28*, 141. (b) Chow, J.; Kopp, R. J.; Portney, P. R. *Science* **2003**, *302*, 1528.

(2) (a) Dresselhaus, M. S.; Thomas, I. L. *Nature* **2001**, *414*, 332. (b) Turner, J. A. *Science* **2004**, *305*, 972. (c) Gray, H. B. *Nat. Chem.* **2009**, *1*, 7.

(3) Walter, M. G.; Warren, E. L.; McKone, J. R.; Boettcher, S. W.; Mi, Q.; Santori, E. A.; Lewis, N. S. *Chem. Rev.* **2010**, *110*, 6446.

(4) (a) Hambourger, M.; Gervaldo, M.; Svedruzic, D.; King, P. W.; Gust, D.; Ghirardi, M.; Moore, A. L.; Moore, T. A. *J. Am. Chem. Soc.* **2008**, *130*, 2015. (b) Le Goff, A.; Artero, V.; Jousselme, B.; Tran, P. D.; Guillet, N.; Métayé, R.; Fihri, A.; Palacin, S.; Fontecave, M. *Science* **2009**, *326*, 1384.

(5) Kundu, A.; Sahu, J. N.; Redzwan, G.; Hashim, M. A. *Int. J. Hydrogen Energy* **2013**, *38*, 1745.

(6) Leroy, R. L. *Int. J. Hydrogen Energy* **1983**, *8*, 401.

(7) For example, see: (a) Razavet, M.; Artero, V.; Fontecave, M. *Inorg. Chem.* **2005**, *44*, 4786. (b) Dempsey, J. L.; Brunschwig, B. S.; Winkler, J. R.; Gray, H. B. *Acc. Chem. Res.* **2009**, *42*, 1995. (c) Losse, S.; Vos, J. G.; Rau, S. *Coord. Chem. Rev.* **2010**, *254*, 2492. (d) Sun, Y.; Bigi, J. P.; Piro, N. A.; Tang, M. L.; Long, J. R.; Chang, C. J. *J. Am. Chem. Soc.* **2011**, *133*, 9212. (e) Artero, V.; Chavarot-Kerlidou, M.; Fontecave, M. *Angew. Chem., Int. Ed.* **2011**, *50*, 7238. (f) McCrory, C. C. L.; Uyeda, C.; Peters, J. C. *J. Am. Chem. Soc.* **2012**, *134*, 3164. (g) Sun, Y.; Sun, J.; Long, J. R.; Yang, P.; Chang, C. J. *Chem. Sci.* **2013**, *4*, 118. (h) King, A. E.; Surendranath, Y.; Piro, N. A.; Bigi, J. P.; Long, J. R.; Chang, C. J. *Chem. Sci.* **2013**, *4*, 1578. (i) Nippe, M.; Khnayzer, R. S.; Panetier, J. A.; Zee, D. Z.; Olaiya, B. S.; Head-Gordon, M.; Chang, C. J.; Castellano, F. N.; Long, J. R. *Chem. Sci.* **2013**, *4*, 3934. (j) Khnayzer, R. S.; Thoi, V. S.; Nippe, M.; King, A. E.; Jurss, J. W.; El Roz, K. A.; Long, J. R.; Chang, C. J.; Castellano, F. N. *Energy Environ. Sci.* **2014**, *7*, 1477.

(8) Andreiadis, E. S.; Jacques, P.-A.; Tran, P. D.; Leyris, A.; Chavarot-Kerlidou, M.; Jousselme, B.; Matheron, M.; Pécaut, J.; Palacin, S.; Fontecave, M.; Artero, V. *Nat. Chem.* **2013**, *5*, 48.

(9) (a) Cobo, S.; Heidkamp, J.; Jacques, P.-A.; Fize, J.; Fourmond, V.; Guetaz, L.; Jousselme, B.; Ivanova, V.; Dau, H.; Palacin, S.; Fontecave, M.; Artero, V. *Nat. Mater.* **2012**, *11*, 802. (b) Sun, Y.; Liu, C.; Grauer, D. C.; Yano, J.; Long, J. R.; Yang, P.; Chang, C. J. *J. Am. Chem. Soc.* **2013**, *135*, 17699.

(10) Kong, D.; Wang, H.; Lu, Z.; Cui, Y. *J. Am. Chem. Soc.* **2014**, *136*, 4897.

(11) Chen, T.; Li, X.; Qiu, C.; Zhu, W.; Ma, H.; Chen, S.; Meng, O. *Biosens. Bioelectron.* **2014**, *53*, 200.

(12) Li, L.; Seng, K. H.; Chen, Z.; Guo, Z.; Liu, H. *Nanoscale* **2013**, *5*, 1922.

(13) Li, Y.; Malik, M. A.; O'Brien, P. *J. Am. Chem. Soc.* **2005**, *127*, 16020.

(14) Popczun, E. J.; Mckone, J. R.; Read, C. G.; Biacchi, A. J.; Wiltrout, A. M.; Lewis, N. S.; Schaak, R. E. *J. Am. Chem. Soc.* **2013**, *135*, 9267.

(15) (a) Pentland, N.; Bockris, J. O. M.; Sheldon, E. *J. Electrochem. Soc.* **1957**, *104*, 182. (b) Conway, B. E.; Tilak, B. V. *Electrochim. Acta* **2002**, *47*, 3571.

(16) Carenco, S.; Portehault, D.; Boissiére, C.; Mézailles, N.; Sanchez, C. *Chem. Rev.* **2013**, *113*, 7981.

(17) Kibsgaard, J.; Chen, Z.; Reinecke, B. N.; Jaramillo, T. F. *Nat. Mater.* **2012**, *11*, 963.

(18) Merki, D.; Fierro, S.; Vrubel, H.; Hu, X. *Chem. Sci.* **2011**, *2*, 1262.

(19) Jaramillo, T. F.; Jørgensen, K. P.; Bonde, J.; Nielsen, J. H.; Horch, S.; Chorkendorff, I. *Science* **2007**, *317*, 100.

(20) Xie, J.; Zhang, H.; Li, S.; Wang, R.; Sun, X.; Zhou, M.; Zhou, J.; Lou, X. W.; Xie, Y. *Adv. Mater.* **2013**, *25*, 5807.

(21) Chen, Z.; Cummins, D.; Reinecke, B. N.; Clark, E.; Sunkara, M. K.; Jaramillo, T. F. *Nano Lett.* **2011**, *11*, 4168.

(22) Grosvenor, A. P.; Wik, S. D.; Cavell, R. G.; Mar, A. *Inorg. Chem.* **2005**, *44*, 8988.

(23) Li, H.; Yang, P.; Chu, D.; Li, H. *Appl. Catal. A: Gen* **2007**, *325*, 34.

(24) Briggs, D., Seah, M. P., Eds. *Practical Surface Analysis by Auger and X-ray Photoelectron Spectroscopy*; John Wiley & Sons: New York, 1983.

(25) Burns, A. W.; Layman, K. A.; Bale, D. H.; Bussell, M. E. *Appl. Catal. A: Gen.* **2008**, *343*, 68.

(26) Yang, Z.; Liu, L.; Wang, X.; Yang, S.; Su, X. *J. Alloys Compd.* **2011**, *509*, 165.

(27) (a) Wilson, A. D.; Shoemaker, R. K.; Miedaner, A.; Muckerman, J. T.; Dubois, D. L.; Dubois, M. R. *Proc. Natl. Acad. Sci. U.S.A.* **2007**, *104*, 6951. (b) Barton, B. E.; Rauchfuss, T. B. *J. Am. Chem. Soc.* **2010**, *132*, 14877.

(28) Nicolet, Y.; de Lacey, A. L.; Vernede, X.; Fernandez, V. M.; Hatchikian, E. C.; Fontecilla-Camps, J. C. *J. Am. Chem. Soc.* **2001**, *123*, 1596.

(29) Liu, P.; Rodriguez, J. A. *J. Am. Chem. Soc.* **2005**, *127*, 14871.

(30) (a) Eyermann, C. J.; Chung-Phillips, A. *J. Am. Chem. Soc.* **1984**, *106*, 7437. (b) Zhang, W.; Wang, Y.; Wang, Z.; Zhong, Z.; Xu, R. *Chem. Commun.* **2010**, *46*, 7631.

(31) Zhang, W.; Hong, J.; Zheng, J.; Huang, Z.; Zhou, J.; Xu, R. *J. Am. Chem. Soc.* **2011**, *133*, 20680.